LOWLAND TECHNOLOGY INTERNATIONAL Vol. 4, No.1, 46-61, June 2002
International Association of Lowland Technology (IALT), ISSN 1344-9656

AN OBSERVATIONAL PREDICTION OF LAND SUBSIDENCE FOR A GIS-AIDED MONITORING SYSTEM OF GROUNDWATER LEVEL

S. Murakami[1], K. Yasuhara[2] and N. Mochizuki[3]

ABSTRACT: A simplified method for observational prediction of land subsidence based on settlement versus time records being previously observed at locations of the objective area was proposed in the present paper for use of the geographical information system (GIS). However, no consideration of ground water level (GWL) variations was taken into proposal of the method. The present paper, however, attempts to realize use of this time series analysis. Settlement variations over time predicted using the proposed two methods available for cases with and without consideration of GWL fluctuation were compared with those observed at locations in the objective area. In comparison with a method which ignores GWL fluctuation, better agreement was recognized between predicted and measured settlement versus time relations. In particular, it was found that the proposed method succeeds in predicting settlement acceleration over time during water shortage periods. Results predicted using the proposed method are displayed as a hazard map using the GIS. Based on the GIS application map, a possible monitoring system is presented for groundwater usage optimization.

INTRODUCTION

Land subsidence remains an important environmental issue, particularly in the extensive plain region in Japan such as the Northern Kanto Plain, Niigata Plain, Nobi plain, or Saga Plain. Land subsidence has induced indirect or compound damage such as submergence during river flooding and earthquake-induced instability of piled foundations as well as direct damage such as uneven settlement of structures. It is very convenient for local government officers and citizens that distribution of possible land-subsidence-induced damage is illustrated in two- or three-dimensional presentations using the Geographical Information System (GIS) (Longley et al. 1999). To realize this, it is essential to adopt simplified procedures, as much as possible, for predicting settlement over a wide area suitable for GIS application. Therefore, a practical procedure for prediction of land subsidence was proposed using previously observed settlement and groundwater level along with elapsed time records combined with the approximate solution of one-dimensional consolidation theory. Parameters included in this method are determined by statistical approximation to observed settlement records and GWL variations over time.

CHARACTERISTICS OF LAND SUBSIDENCE IN THE NORTHERN KANTO PLAIN

Figures 1 and 2 demonstrate the objective area, which is called the Northern Kanto Plain, covering the five prefectures of Saitama, Gunma, Tochigi, Ibaraki, and Chiba including locations where variations of settlement and GWL over time have been observed in the past

1 Research Associate, Department of Urban and Civil Engineering, Ibaraki University, JAPAN.
2 Professor, Department of Urban and Civil Engineering, Ibaraki University, JAPAN.
3 Graduate student, School of Science and Technology, Ibaraki University, Ibaraki, JAPAN.
Note: Discussion on this paper is open until December 25, 2002.

20 years. Settlement in this area has been caused by groundwater abstraction for industrial, drinking, and agricultural purposes. In the area, they suffer from approximately several centimeters as the annually average value of settlement. Settlement over this area occupies 80% of total settlement area in land subsidence of Japan. Land subsidence features in this area indicated in the previous paper (Murakami et al. 1998) are characterized by the following:

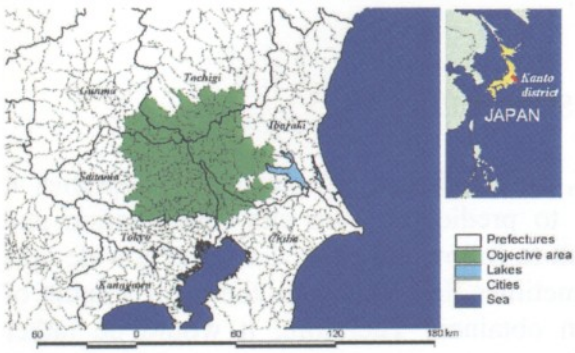

Fig. 1 Objective area for land subsidence in the Northern Kanto Plain in Japan

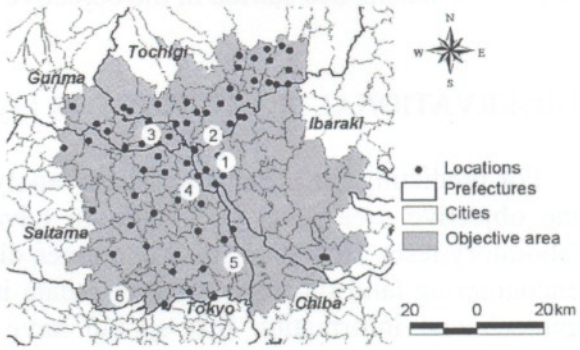

Fig. 2 Objective area for land subsidence with locations of settlements and groundwater level measurements

1) Rate of settlement in the southwest region of Saitama, where they were marked in late 1970, tends to become calm; and

2) Markedly prevailed area of land subsidence has shifted from the border between Saitama and Ibaraki to the area covering the three prefectures of Tochigi, Ibaraki, and Saitama.

Figure 3 illustrates variations of observed settlement and GWL over time at representative locations in the objective area, which are indicated by white circled numbers in Fig. 2. Groundwater abstraction for industrial and drinking purposes are performed continuously. On the other hand, abstraction for agricultural purpose is done seasonally. Therefore, GWL in the area fluctuates seasonally in the manner where the GWL falls due to continuous abstraction, and settlement progresses with elapsed time under the approximately constant frequency with the GWL fluctuation. However, larger GWL variation does not necessarily produce increase in larger settlements. The reasons for this phenomenon are that thickness and compressibility of layers, and the amount of settlement, which has taken place before measurement started, are different from each location.

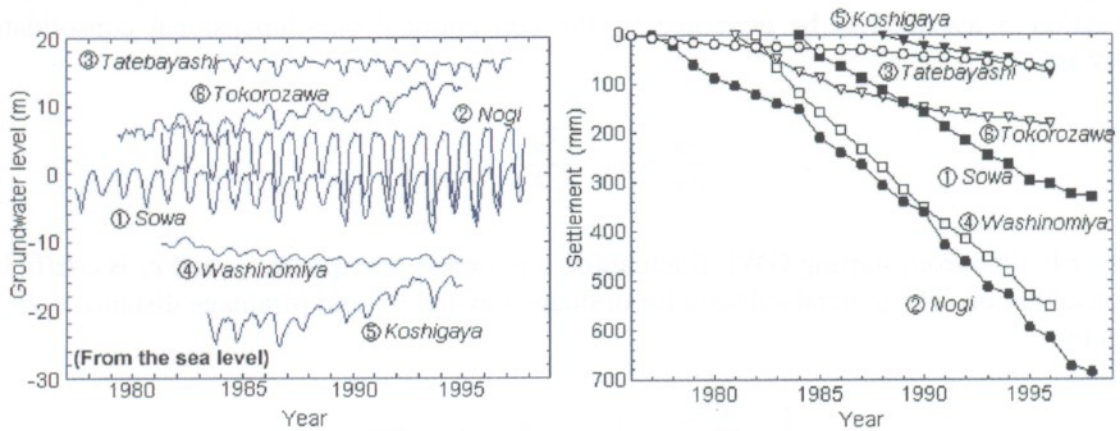

Fig. 3 Variations of settlement and groundwater level with elapsed time

The conventional one-dimensional consolidation theory indicates that settlement due to land subsidence relies not only on external forces, but also on soil profiles and geotechnical properties in the existing area, as seen in the case of Sowa in Ibaraki in Fig. 3. Settlement may have already taken place in some locations before measurement started. Therefore, it is important to detect the future relations between settlements versus time by extrapolation, since land subsidence started in the objective area.

OBSERVATIONAL PREDICTION FOR LAND SUBSIDENCE

For predicting settlements as "direct analysis", soil profiles and geotechnical properties at the objective area must be known in advance to prediction from site investigation and laboratory tests. However, it is sometimes difficult to follow this procedure over a wide area encountering land subsidence because data is sometimes limited despite the great amount of geotechnical information that should have been obtained. Therefore, it would be rather convenient to predict relations of settlement and elapsed time by making use of settlement and groundwater level in comparison with time records previously observed available at the objective site. This procedure might be classified as "inverse analysis" or back calculation.

Fortunately, in general there are many locations in which variations of settlement and GWL fluctuation over time have been measured at the land subsidence area. Therefore, an observational procedure is presented for predicting relations of settlement versus time under the constant range in GWL variation and GWL fluctuation in the Northern Kanto plain.

OBSERVATIONAL PREDICTION WITHOUT CONSIDERATION OF GWL FLUCTUATION

Fundamental Equation for a Simplified Observational Prediction

A first attempt was made to predict relations of future settlement versus elapsed time based on land subsidence-time records previously measured at locations as shown in Fig. 1. However, since the method was already described in the previous paper (Murakami et al. 1998, 2000a, 2000b), following is a brief procedural review:

Figure 4 illustrates a settlement set and relation of GWL against time. Although external load given by Δh varies with time, here accumulated settlement at every cycle of GWL fluctuation is assumed to be governed by the conventional one-dimensional consolidation theory as:

$$\frac{\partial u}{\partial \tau} = c_v \frac{\partial^2 u}{\partial z^2} \tag{1}$$

where τ is time from starting GWL fluctuation, u is excess pore pressure, and c_v is coefficient of consolidation. The general solution for drainage top and bottom (drainage distance is H_d) is given by:

$$\Sigma = \Sigma_f \left\{ 1 - \sum_{n=1}^{\infty} \frac{2}{a_n^2} exp\left(- a_n^2 T_v \right) \right\}, \left(a_n = \frac{2n-1}{2} \pi \text{ ;n=1,2,3,...} \right) \tag{2}$$

where Σ is settlement from starting GWL fluctuation, Σ_f is the final settlement, and T_v is time factor as defined by:

$$T_v = \frac{c_v}{H_d^2}\tau \tag{3}$$

When we consider the interval between two time factors of T_{v0} and T_{vi}, which relate to τ_0 and τ_i, respectively, the settlement difference S_i yields:

$$S_i = \Sigma_i - \Sigma_0 = \Sigma_f \cdot \sum_{n=1}^{\infty}\left[\frac{2}{a_n^2}exp\left(-a_n^2 T_{v0}\right)\left\{1 - exp\left\{-a_n^2\left(T_{vi} - T_{v0}\right)\right\}\right\}\right] \tag{4}$$

Using Eq. (3), $T_{vi} - T_{v0}$ in Eq. (4) can be expressed as :

$$T_{vi} - T_{v0} = \frac{c_v}{H_d^2}\left(\tau_i - \tau_0\right) = \frac{c_v}{H_d^2}t_i \tag{5}$$

where t_i is time from the beginning of measuring settlement. By neglecting the difference in inherent values after the second order in the consolidation theory solution , Eq. (4) leads to:

$$S_i = \Sigma_f \frac{8}{\pi^2}exp\left(-\frac{\pi^2}{4}T_{v0}\right)\left\{1 - exp\left(-\frac{\pi^2}{4}\frac{c_v}{H_d^2}t_i\right)\right\} \tag{6}$$

where S_i is accumulated settlement from the beginning of measuring settlement to t_i. Let us here assume that :

$$S_{p0} = \Sigma_f \frac{8}{\pi^2}exp\left(-\frac{\pi^2}{4}T_{v0}\right), C_R = \frac{\pi^2}{4}\frac{c_v}{H_d^2} \tag{7}$$

where S_{p0} is the residual settlement expected from the present time until the termination of subsidence under the assumption that the groundwater variation is kept the same as observed at the present time and C_R is a parameter corresponding to settlement strain rate. Substitution of Eq. (7) into Eq. (6) yields :

$$S_i = S_{p0}\left\{1 - exp\left(-C_R \cdot t_i\right)\right\} \tag{8}$$

As the general form instead of Eq. (8), suitable for an arbitrary time we have:

$$S = S_{p0}\left\{1 - exp\left(-C_R \cdot t\right)\right\} \tag{9}$$

The concrete values of two parameters given by Eq. (7) . These are determined by using the non-linear least squares method which should satisfy the following (Murakami et al. 1998):

$$\partial F_1 / \partial S_{po} = 0, \quad \partial F_1 / \partial C_R = 0 \tag{10}$$

where F_1 is given as:

$$F_1 = \sum_{i=1}^{n} \left[S_i^m - S_{po} \{1 - exp(-C_R \cdot t_i)\} \right]^2 \qquad (11)$$

in which S_i^m is the observational settlement at t_i. A family of data of S_{p0} and C_R for typical locations at the objective area was adopted for forecasting future settlement variation with elapsed time through previously recorded land subsidence.

OBSERVATIONAL PREDICTION WITH CONSIDERATION OF GWL FLUCTUATION

Basic Equation

To consider the effect of GWL fluctuation when forecasting settlement due to groundwater abstraction, time series analysis was adopted and results were combined with the method with no consideration of GWL fluctuation which was presented in the previous chapter (Murakami et al. 2001). The predictive procedure is described in the followings

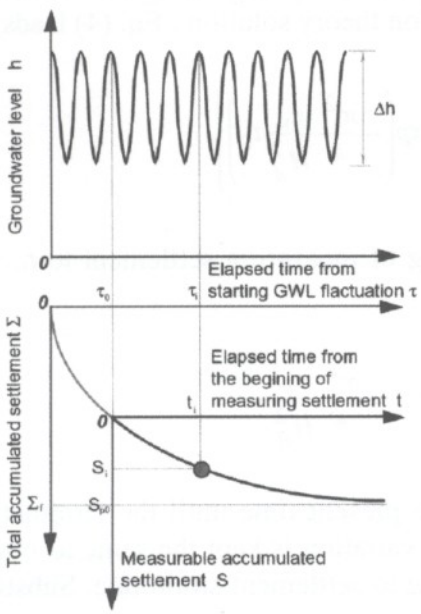

Fig. 4 Settlement versus elapsed time curve

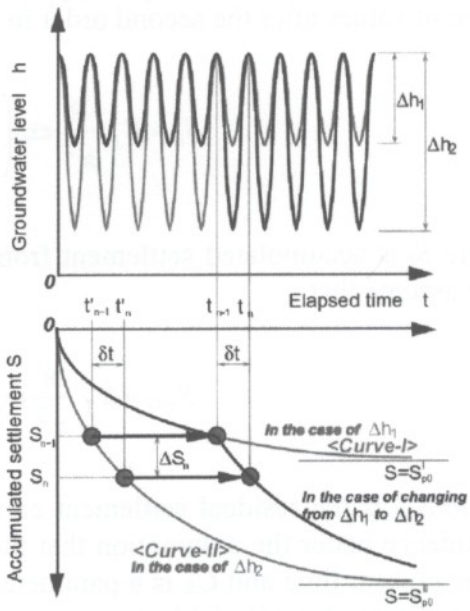

Fig. 5 Change of Settlement versus elapsed time curve

1) Figure 5 schematically illustrates two curves for GWL variation over time under different GWL fluctuation with Δh_1 and Δh_2 ($\Delta h_1 < \Delta h_2$). Expressing possible residual settlement, corresponding to the year, to start measurements of land subsidence and groundwater level as S_{po}^{II}, S_{po}^{I}, then we have:

$$S^I = S_{p0}^{\ I} \{1 - exp(-C_R \cdot t)\} \quad (\text{in the case of } \Delta h = \Delta h_1) \qquad (12a)$$

$$S^{II} = S_{p0}^{\ II} \{1 - exp(-C_R \cdot t)\} \quad (\text{in the case of } \Delta h = \Delta h_2) \qquad (12b)$$

2) We assume that curve I is shifted to curve II for settlement against time relations when the groundwater level fluctuation changes from Δh_1 to Δh_2, then incremental settlement δS_n from time interval δt ($= t_n' - t'_{n-1}$) is given below :

$$\Delta S_n = S_n - S_{n-1} = S_{p0}^{II} \exp(-C_R t'_{n-1})\{1 - \exp(-C_R \cdot \delta t)\} \tag{13}$$

Here we have

$$S_{p0}^{II} \exp(-C_R \cdot t'_{n-1}) = S_{p0}^{II} - S_{n-1} \tag{14}$$

then Eq. (13) is rewritten as the following equation :

$$\Delta S_n = S_n - S_{n-1} = \left(S_{p0}^{II} - S_{n-1}\right)\{1 - \exp(-C_R \cdot \delta t)\} \tag{15}$$

In the case of δt = 1 year, Eq. (15) yields Eq. (16) :

$$\Delta S_n = \left(S_{p0}^{II} - S_{n-1}\right)\{1 - \exp(-C_R)\} \tag{16}$$

The important parameter S_{p0} must depend on groundwater characteristics, particularly the GWL fluctuation range. Therefore, as shown in Fig. 6, let us assume here that S_{p0} is linearly correlated with Δh as:

$$S_{p0} = A_w \cdot \Delta h + B_w \tag{17}$$

Then, an incremental settlement, ΔS_n, is given by

$$\Delta S_n = A \cdot \Delta h_n + B \cdot S_{n-1} + C \tag{18}$$

where A, B and C are:

$$A = A_w\{1 - \exp(-C_R)\},\ B = -\{1 - \exp(-C_R)\},\ C = B_w\{1 - \exp(-C_R)\} \tag{19}$$

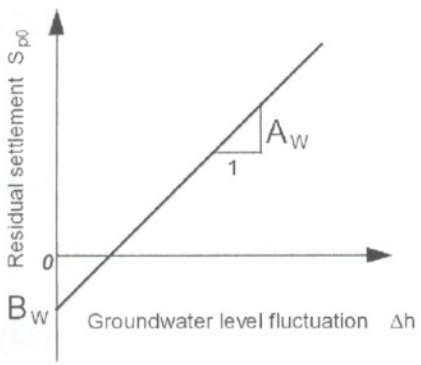

Fig. 6 Δh and S_{p0} relation

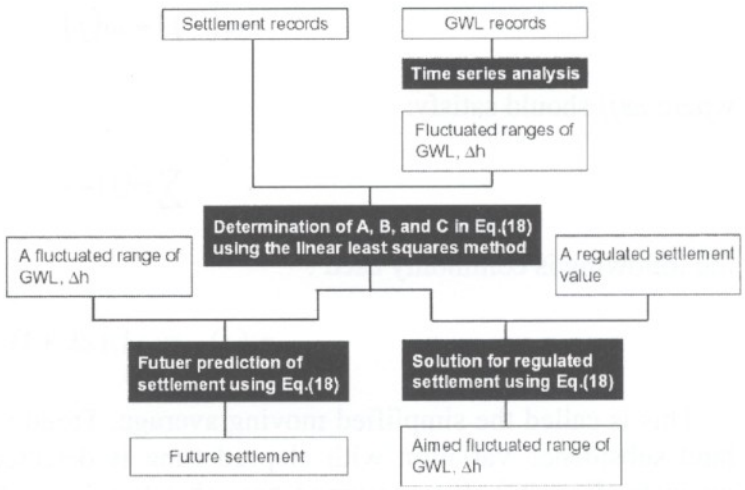

Fig. 7 A flow chart for a prediction of a settlement and an aimed fluctuated range of GWL

Determination of A, B and C

Values of A, B and C are determined by minimizing function F_2, which is expressed by:

$$F_2 = \sum_{n=1}^{N} \left[\Delta S_n^m - \left(A \cdot \Delta h_n + B \cdot S_{n-1}^m + C \right) \right]^2 \tag{20}$$

Minimization of Eq. (20) is equivalent to satisfy the following relation:

$$\frac{\partial F_2}{\partial A} = \frac{\partial F_2}{\partial B} = \frac{\partial F_2}{\partial C} \tag{21}$$

Although Appendix A describes detail, at least three sets of data are needed for settlement prediction using the linear least squares method as stated above.

Determination of Range in Groundwater Level Fluctuation

It is essential to consider GWL fluctuation for improving a method of predicting land subsidence. To determine amount of GWL fluctuation, time series analysis was adopted and proved by application to previously observed GWL variations over time. The procedure is described in the following:

1) By regarding the GWL's records as time series data, $h(t)$, trend analysis was carried out and estimated value of trend variation, $m(t)$, was detected. This is a milestone for determining range of GWL fluctuation.

2) As a time series analysis for determining range in GWL fluctuation, we employed a moving average that is equivalent to an average value for k with weighting before and after the centered value at a certain time, t. Although this time series analysis needs to classify GWL fluctuation into the trend and random components, the k-value should be determined in order to eliminate the random component. If weight multiplied at a time of $t+j$ ($-k \quad j \quad k$) is assumed $\omega(j)$, trend variation predicted by moving variation is generally expressed as:

$$\omega(-j) = \omega(j) \tag{22}$$

where $\omega(j)$ should satisfy:

$$\sum \omega(j) = 1 \tag{23}$$

the following is commonly used :

$$\omega(j) \quad = \quad 1/(2k+1) \tag{24}$$

This is called the simplified moving average. Trend variation in GWL used for estimating land subsidence variation with elapsed time is detected using the simple moving average given by Eq. (22). It is assumed here that trend variation is determined from the moving average that is estimated using data measured for every 12 months because GWL for the objective area varies with almost one frequency per a year. The following is the procedure for this detection.

1) By postulating k equal to 6, determine a moving average of the 12 terms, $\hat{h}$. That is, we have:

$$\hat{h}(t-0.5)=\{h(t-6)+h(t-5)+\cdots+h(t)+\cdots h(t+5)\}/12 \tag{25}$$

2) Calculate the average of the moving average given by Eq. (25), and then set a presumed value, $m(t)$, of the trend component included in time series analysis which is expressed by:

$$m(t)=\{\hat{h}(t-0.5)+\hat{h}(t+0.5)\}/2 \tag{26}$$

3) Calculate difference between presumed value, $m(t)$, and measured value, $h(t)$. Then, detect location (z_1, z_2), which exhibits the largest difference of GWL.

$$z_1=\max[h(t)-m(t)],\ z_2=\min[h(t)-m(t)] \tag{27}$$

4) Finally, by assuming that the fluctuated range of GWL, Δh, should be equal to the sum of distances from the presumed value in trend variation, we obtain:

$$\Delta h=z_1-z_2 \tag{28}$$

The fluctuated value of GWL estimated using Eq. (28) becomes equivalent to an external force which induces land subsidence. Thus, amount of settlement and settlement versus elapsed time relations can be predicted.

Application of Time Series Analysis to Land Subsidence Prediction

Applicability of the proposed land subsidence prediction procedure that considers GWL fluctuation is proved by using Eq. (18) combined with Eq. (27). Data of GWL variations and movement of ground surface, which have been measured in these twenty years in the objective area, are used for this purpose. The prediction procedure is summarized in Fig. 7 as a flow chart.

Black circles in Fig. 2 indicate locations where GWL variations and ground surface movement over time have been measured. Figure 8 shows the measuring system for both data. The typical set of settlement versus time relations measured at the representative six locations is compared with those calculated by using Eq. (18) with Eq. (28) and by following the procedure in Fig. 7. Overall good agreement is observed in measured and calculated variations of GWL over time. As an example among them, a further comparison is made for the case of Nogi in Tochigi Prefecture, between settlement versus time relations observed calculated using two methods with and without consideration of GWL fluctuation. It can be said from a comparison in Fig. 9 that the improved method with consideration is more accurate than the original method without consideration of GWL fluctuation, even where a suddenly increased GWL variation, as seen in Fig. 10 for the case of Nogi, occurs due to water shortage during the dry season. To ensure overall validity of Eq. (18) with Eq. (27), the multi-correlation coefficient is detected from settlement versus time relations calculated and observed for the three years from 1992 through 1994. Coefficients for 72 locations detected are plotted in Fig. 11 against measured settlement for three years. The correlation coefficient is as high as 0.85 for most cases beyond measured settlement of 15 mm except the four locations with small settlement amount measured where the coefficient is lower than 0.6.

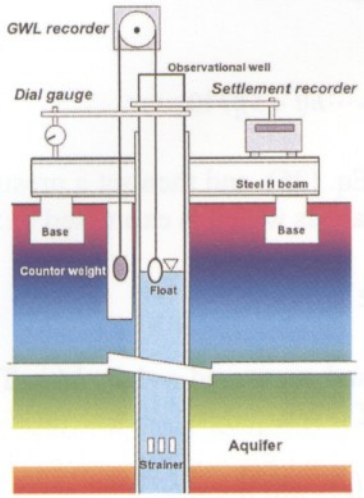

Fig. 8 A measuring system for settlement and GWL data

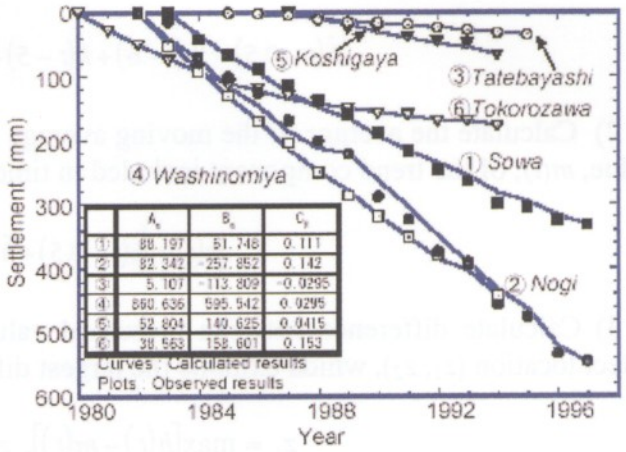

Fig. 9 Comparison between observed settlement and calculated results versus time relation

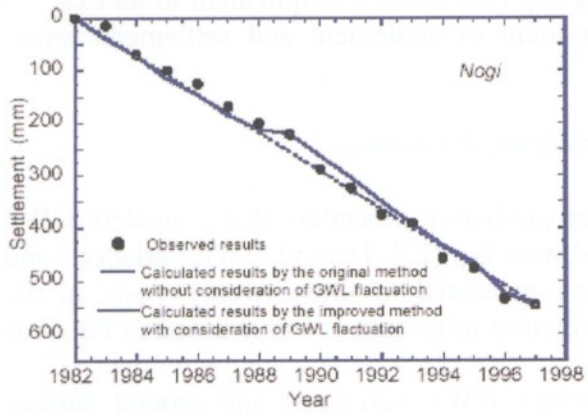

Fig. 10 Comparison between two methods with and without consideration of GWL flactuation

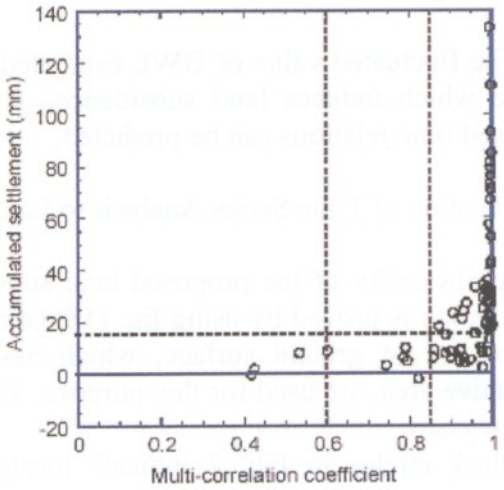

Fig. 11 Accumulated settlement versus multiple-correlation coefficient relations

VISUALIZATION OF PREDICTED LAND SUBSIDENCE AND DAMAGE POTENTIAL

Display of Land Subsidence

Following the above-mentioned procedure, settlement prediction during 1998 to 2002 was conducted using previously observed settlement versus time records observed at objective areas. Influence of GWL fluctuation was investigated in the three cases of the average, 2/3 and 1/2 of the average of fluctuation being assumed, which was observed during 1990 to 1994. Total settlement was estimated using Eq. (18) in which values of A, B and C included were determined using the same minimum square method as used in the previous section.

Subsequently, the settlement database for all discrete locations was constructed by combining coordinate data where location data was input from the digitizer. Among this database, observed data in which values of A_w and C_R included in Eq. (18) and Eq. (8) were less than 0 was excluded for prediction. Using data from 49 locations after exclusion, GIS was used for presenting the predicted results two-dimensionally for easy visualization of distribution in the vast area under investigation. Unavailable data was interpolated in the UTM coordinate and discrete data was transformed into the square mesh with 1 km x 1 km. For interpolation of these data, the Kriging method (Deutch and Journel 1998), which is commonly used in the field of spatial information science, was adopted because it was capable of demonstrating spatial relations which give influence of distance and direction between sample points on surface expression. Figure 12 shows planar distribution of predicted settlement in three cases of GWL fluctuation being assumed together with the border lines of prefectures, cities, and towns. The following can be indicated from Fig. 12:

1) When land subsidence continues under average values of GWL fluctuation measured during 1990 to 1994 being adopted, settlement predicted during the 10 years from 1995 through 2004 become larger in the vicinity of the border between Saitama and Ibaraki than in other area. This suggests that it is necessary to take some countermeasures for regulating groundwater abstraction in this area.

2) In the case of assuming regulated GWL fluctuation to a half of the average value observed during 1990 though 1994, swelling of 200 mm takes place although predicted settlement is, at most, 100 mm around the area of Nogi in Tochigi, under the same GWL fluctuation as the average value measured during 1990 to 1994. Although this is unrealistic, it can be said at least that ground surface displacement around Nogi is strongly influenced by GWL fluctuation. This is probably due to the existing thick, soft, and compressible clay layer. This should be confirmed by site investigation in Nogi and its vicinity from a geological and geotechnical point of view.

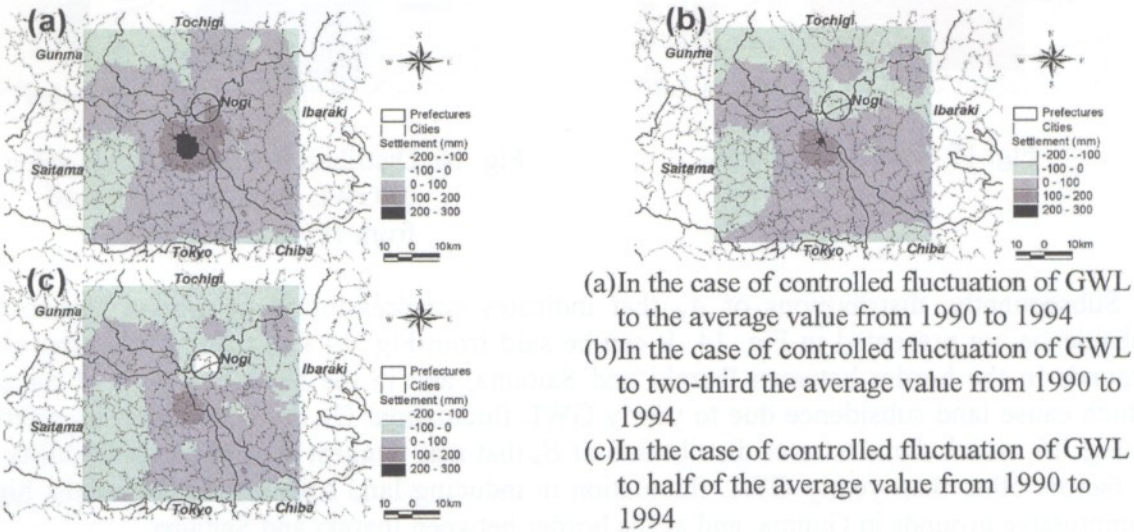

(a)In the case of controlled fluctuation of GWL to the average value from 1990 to 1994
(b)In the case of controlled fluctuation of GWL to two-third the average value from 1990 to 1994
(c)In the case of controlled fluctuation of GWL to half of the average value from 1990 to 1994

Fig. 12 Distribution of predicted land subsidence (1995-2004)

Distribution of Parameters Contributing to Land Subsidence

As previously described, the three parameters, A_w, B_w and C_R included in Eq. (18) correspond to compressibility due to yearly GWL fluctuation, compressibility due to other factors, and rate of settlement, respectively. This means that those parameters represent settlement characteristics in the land subsidence area. Based on GWL fluctuation monthly

data and yearly surface displacement observed at the 49 locations in the northern Kanto plain, those three parameters were determined. Their distribution was displayed using GIS. Planar representation using GIS was done on the UTM coordinates where interpolation was applied in terms of the Kriging method; and raster data with 1 km square was produced.

Progressive characteristics of land subsidence are described with the parameter C_R. In other words, the larger C_R becomes, the more rapidly land subsidence progresses and the earlier land subsidence terminates, and vice versa. Figure 13 demonstrates distribution of this C_R in the objective area. It is understood that land subsidence has a tendency to become prolonged in the wide region except all over Saitama, southern part of Tochigi, and a part of Chiba and neighboring Ibaraki.

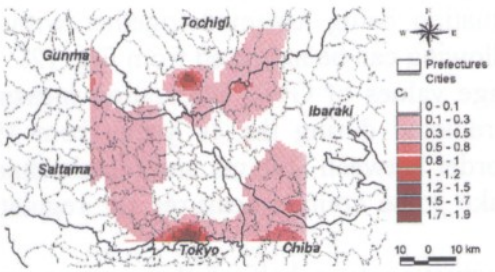

Fig.13 Distribution of C_R

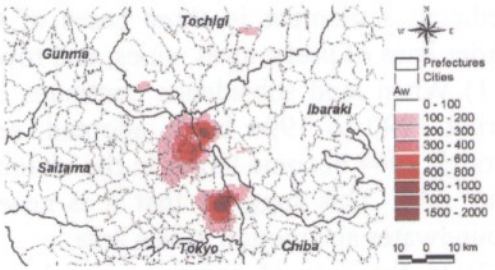

Fig.14 Distribution of A_w

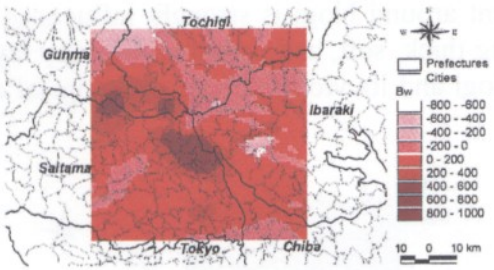

Fig. 15 Distribution of B_w

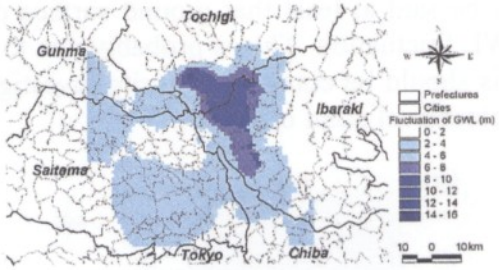

Fig. 16 Distribution of the average value of GWL fluctuation observed from 1990 to 1994

Subsequently, distributions of A_w that indicates compressibility of ground due to land subsidence are presented in Fig. 14. It can be said from Fig. 14 that there exist compressive grounds in the border between Ibaraki and Saitama, and in the south-east area of Saitama, which cause land subsidence due to yearly GWL fluctuation. On the other hand, by referring to Fig. 15, which demonstrates distribution of B_w that may suggest ground compressibility due to factors other than yearly GWL fluctuation in inducing land subsidence, there exist highly compressive grounds in Gunma, and at the border between Ibaraki and Saitama.

It is necessary to analyze the present land subsidence situation using respective values of the three parameters, C_R, A_w and B_w, to grasp characteristics of time-dependent GWL fluctuation. Figure 16 illustrates planar distribution of average values of GWL fluctuation that were measured during the five years from 1990 to 1994.

Presentation of Damage Potential due to Land Subsidence

Land subsidence-induced damage is divided into direct and indirect varieties (Murakami et al. 1998; Yasuhara and Murakami 2001). Types of damage caused by land subsidence,

however, are different for each site in the objective area because site characteristics differ depending on geographical and geomorphologic situation. For example, water supply for irrigation deteriorates in agricultural areas. Bearing capacity of ground supporting structures with pile foundations may induce inclination and underground services may be damaged in industrial and business areas (Yasuhara and Murakami 2001). Therefore, site characteristics must be considered to estimate possible damage caused by land subsidence.

Damage potential D_p at a site is defined by summation of products of the degree of damage D_i and weighting w_i and is given by:

$$D_p = \sum_{i}^{N} w_i D_i \tag{29}$$

For simplicity, D_i, is assumed to be given by the following equation:

$$D_i = d_i / d_{\max} \tag{30}$$

where d_i and d_{max} are given by:

$$d_i = A_i S_i \tag{31}$$

$$d_{\max} = \max\{d_i\} \tag{32}$$

In Eq. (31), A_i is the damaged area , S_i is future settlement in a site being given by Eq. (8), and d_{max} is the maximum value of d_i in the objective area.

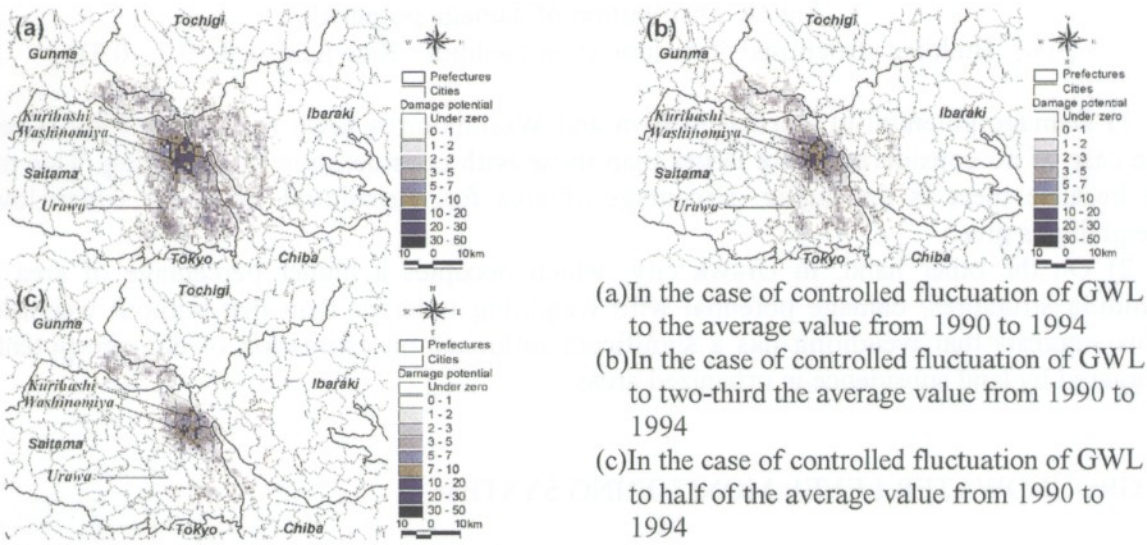

(a)In the case of controlled fluctuation of GWL to the average value from 1990 to 1994
(b)In the case of controlled fluctuation of GWL to two-third the average value from 1990 to 1994
(c)In the case of controlled fluctuation of GWL to half of the average value from 1990 to 1994

Fig.17 Distribution of damage potential
(w_i; Building structures : Transportation facilities : Rice field=1.0 : 1.0 : 1.0)

Using the above, an attempt has been made to draw a damage potential map using GIS. Built up areas and rice fields obtained from a database of existing regional information were used for the damaged area A_i and predicted settlement amounts, obtained from Fig. 12, were used as future settlement values, S_i. A case of weighting, w_i, is assumed to be 1.0, 0.7, and 0.3 for sites for building structures, transportation facilities, and agricultural fields, respectively.

Estimated results for damage potential in the case without considering weighting, that is to say, assuming w_i equal to unity for all sites, are presented in Fig. 17. Occurrence of damage caused by land subsidence for each site can be specified by means of this map rather than a mere future settlement map. Results of the case considering weight for the categorized three representative sites are shown in Fig. 18. Overall, no significant difference has been observed in damage potential distribution between two cases with and without consideration of weight, depending on the manner of site utilization under consideration: e.g., for buildings, bridges, or rice fields. However, the following characteristic features are seen from observation of individual details in Fig. 18:

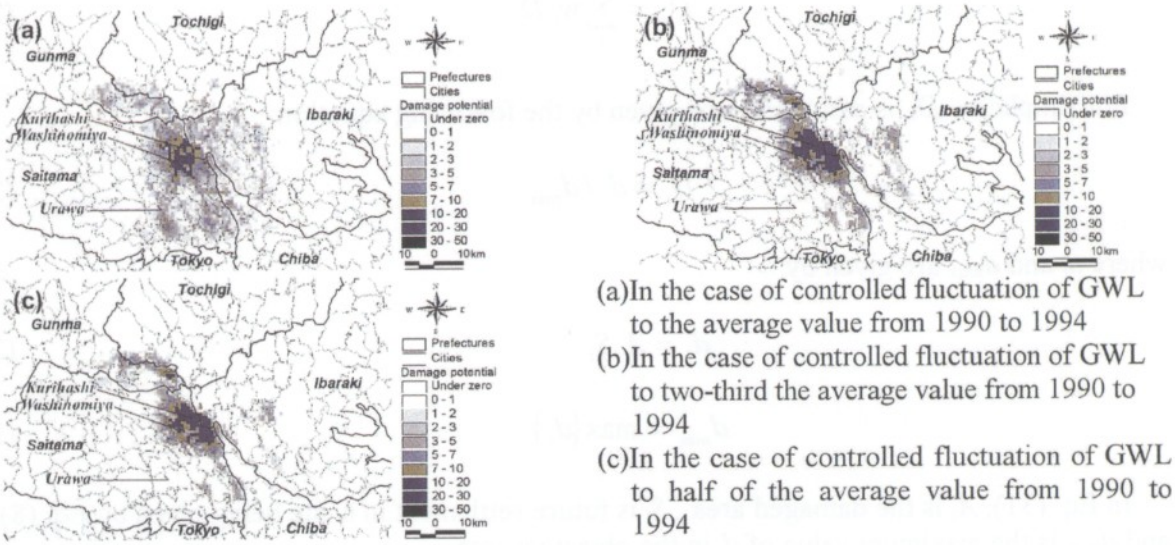

(a)In the case of controlled fluctuation of GWL to the average value from 1990 to 1994

(b)In the case of controlled fluctuation of GWL to two-third the average value from 1990 to 1994

(c)In the case of controlled fluctuation of GWL to half of the average value from 1990 to 1994

Fig.18 Distribution of damage potential
(w_i; Building structures : Transportation facilities : Rice field=1.0 : 0.7 : 0.3)

1) Damage potential in Kurihashi town and Washinomiya town in Saitama Prefecture in the case of no consideration are larger than those with consideration of weighting. This may be because there is the higher percentage of area for agricultural fields for which lower weighting is given.

2) On the other hand, in Urawa city, which occupies a higher percentage of area for building structures, damage potential with weighting is larger than that without weighting. This suggests that weighting has a significant influence on estimation of damage potential triggered by land subsidence in urbanized areas.

A GROUNDWATER LEVEL MONITORING SYSTEM

In order to reduce direct and indirect damage due to land subsidence, GWL should be systematically monitored and transmitted to users from time to time. An example of this kind of monitoring system has been developed by the Saitama prefecture local government (Satoh et al. 2000). This is schematically illustrated in Fig. 15 together with location of a GIS system proposed by the authors based on results of the following evaluation followed using GIS.

Figures 19 a,b and c demonstrate GWL fluctuation distribution calculated by assuming 20 mm, 10 mm, and zero as regulated settlement values. The calculated amount of allowable GWL fluctuation becomes smaller as assumed annual settlement decreases. Results in Fig. 19 show that the area most sensitive to fluctuation is the belt area near Nogi in Tochigi. It is

peculiar that calculated GWL fluctuation in the case of regulated settlement being zero is less than zero in the area from Gunma to eastern Saitama. From a viewpoint of geotechnical engineering, this phenomenon should not appear. Therefore, it is concluded that it is impossible to regulate to annual settlement zero for this area. Judging entirely from above-stated trends, Fig. 19 with GIS-aided only shows the aimed value which should not exceed beyond that for regulating settlement for each location to a required value.

It is concluded from the above-stated consideration that advantageous features using GIS for monitoring settlement and GWL are:

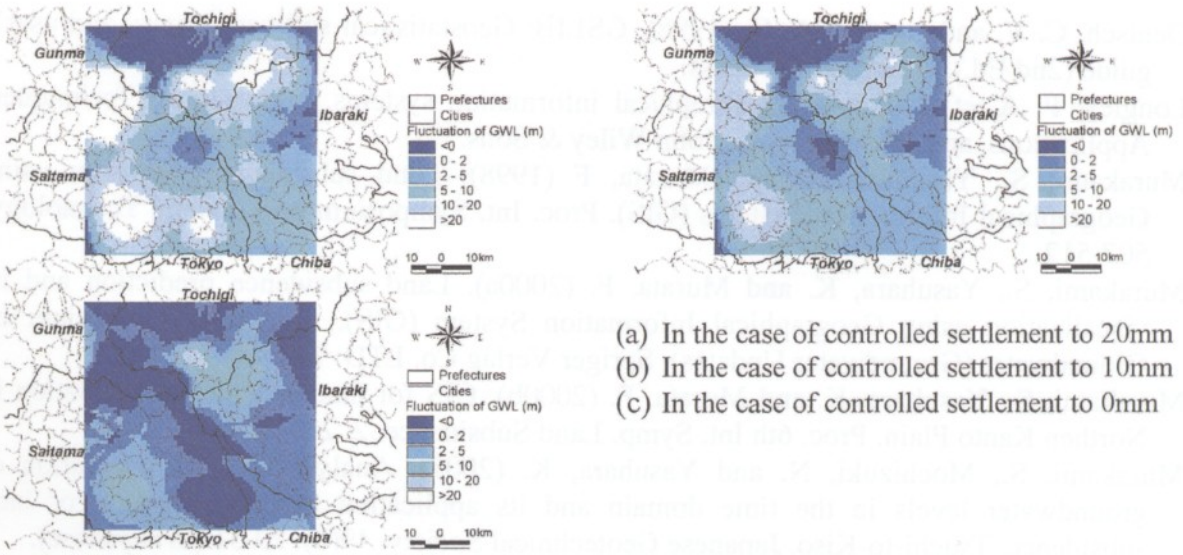

(a) In the case of controlled settlement to 20mm
(b) In the case of controlled settlement to 10mm
(c) In the case of controlled settlement to 0mm

Fig.19 Predicted fluctuation of GWL for controlled settlement (1996)

1) It is possible to specify areas in which predicted land subsidence is severe under constant GWL variation continuing, and areas where influence of GWL regulation on land subsidence is eminent;

2) Severity of influence of GWL regulation on land subsidence can be ascertained for each site and areas requiring or benefitting from countermeasures are identified; and

3) It must be possible to control land subsidence corresponding to site characteristics by setting up GML target values for the required value of settlement and by performing more careful monitoring. Based on this idea, a practical monitoring system using GIS may be proposed in the near future.

CONCLUSIONS

A simplified method of observational prediction for land subsidence based on settlement versus time records being previously observed at locations of the objective area was proposed in the previous paper for use of geographical information system (GIS). However, no consideration of ground water level (GWL) variation was taken into the method. In the present paper, therefore, an effort was made to consider of GWL fluctuation successfully using time series analysis. Subsequently, predicted settlement variations over time using methods proposed for cases with and without consideration of GWL fluctuation were compared with those observed at approximately 100 locations at the Northern Kanto plain which have suffered the most severe land subsidence in Japan. By considering GWL fluctuation, good agreement was recognized between predicted and measured settlement

versus time. In particular, it is clear that the method even succeeds in predicting settlement acceleration over time during the dry season. Results predicted using the proposed method are presented as a hazard map using GIS. Based on the GIS-assisted map display, a possible GWL monitoring system is presented through optimization for groundwater abstraction for individual application in each area.

REFERENCES

Deutsch, C. V. and Journel, A. G. (1998). GSLIB: Geostatistical software library and user's guide (2nd Ed.). Oxford Univ. Press.

Longley, P. A. et al. (1999). Geographical information systems, - Principles, Techniques, Applications, and Management -. John Wiley & Sons.

Murakami, S., Yasuhara, K. and Murata, F (1998). Land subsidence prediction using Geographical Information Systems (GIS). Proc. Int. Symposium on Lowland Technology: 507-512.

Murakami, S., Yasuhara, K. and Murata, F. (2000a). Land subsidence prediction and its visualization using Geographical Information System (GIS). Proc. Int. Symposium on Groundwater (Groundwater Updates), Spriger Verlag Co. LTD: 79-84.

Murakami, S., Yasuhara, K. and Murata, F. (2000b). GIS for land subsidence evaluation in Northen Kanto Plain. Proc. 6th Int. Symp. Land Subsidence. 2: 219-228.

Murakami, S., Mochizuki, N. and Yasuhara, K. (2001). Analyses of the fluctuation of groundwater levels in the time domain and its application to the prediction of land subsidence, Tsuchi-to-Kiso, Japanese Geotechnical Society. 49(6): 29-31 (in Japanese).

Sato, K. (2000). A new control system of groundwater resource. Proc. Int. Symposium on Groundwater (Groundwater Updates), Spriger Verlag Co. LTD.: 13-16.

Yasuhara, K. and Murakami, S. (2001). GIS for seismic risk evaluation of piled foundation in land subsidence area. Proc. 15th ICSMGE. 2 : 1043-1046.

APPENDIX : Determination of A, B and C

By solving Eq. (21), we have:

$$\sum_{n=1}^{N} \Delta h\left(A \cdot \Delta h + B \cdot S_{n-1} + C\right) = \sum_{n=1}^{N} \Delta h \cdot \delta S_n$$

$$\sum_{n=1}^{N} S_{n-1}\left(A \cdot \Delta h + B \cdot S_{n-1} + C\right) = \sum_{n=1}^{N} S_{n-1} \cdot \delta S_n \qquad \text{(i)}$$

$$\sum_{n=1}^{N} \left(A \cdot \Delta h + B \cdot S_{n-1} + C\right) = \sum_{n=1}^{N} \delta S_n$$

Hence, Eq. (i) yields:

$$\begin{pmatrix} \Delta h_1 & \Delta h_2 & \cdots & \Delta h_N \end{pmatrix} \begin{Bmatrix} \Delta h_1 & S_0 & 1 \\ \Delta h_2 & S_1 & 1 \\ \vdots & \vdots & \vdots \\ \Delta h_N & S_{N-1} & 1 \end{Bmatrix} \begin{Bmatrix} A \\ B \\ C \end{Bmatrix} = \begin{pmatrix} \Delta h_1 & \Delta h_2 & \cdots & \Delta h_N \end{pmatrix} \begin{Bmatrix} \delta S_1 \\ \delta S_2 \\ \vdots \\ \delta S_N \end{Bmatrix} \qquad \text{(ii)}$$

$$\begin{pmatrix} S_1 & S_2 & \cdots & S_N \end{pmatrix} \begin{Bmatrix} \Delta h_1 & S_0 & 1 \\ \Delta h_2 & S_1 & 1 \\ \vdots & \vdots & \vdots \\ \Delta h_N & S_{N-1} & 1 \end{Bmatrix} \begin{Bmatrix} A \\ B \\ C \end{Bmatrix} = \begin{pmatrix} S_1 & S_2 & \cdots & S_N \end{pmatrix} \begin{Bmatrix} \delta S_1 \\ \delta S_2 \\ \vdots \\ \delta S_N \end{Bmatrix} \quad \text{(iii)}$$

$$\begin{pmatrix} 1 & 1 & \cdots & 1 \end{pmatrix} \begin{Bmatrix} \Delta h_1 & S_0 & 1 \\ \Delta h_2 & S_1 & 1 \\ \vdots & \vdots & \vdots \\ \Delta h_N & S_{N-1} & 1 \end{Bmatrix} \begin{Bmatrix} A \\ B \\ C \end{Bmatrix} = \begin{pmatrix} 1 & 1 & \cdots & 1 \end{pmatrix} \begin{Bmatrix} \delta S_1 \\ \delta S_2 \\ \vdots \\ \delta S_N \end{Bmatrix} \quad \text{(iv)}$$

Eq. (ii),(iii),(iv) can be rewritten into:

$$\begin{pmatrix} \Delta h_1 & \Delta h_2 & \cdots & \Delta h_N \\ S_0 & S_1 & \cdots & S_{N-1} \\ 1 & 1 & \cdots & 1 \end{pmatrix} \begin{Bmatrix} \Delta h_1 & S_0 & 1 \\ \Delta h_2 & S_1 & 1 \\ \vdots & \vdots & \vdots \\ \Delta h_N & S_{N-1} & 1 \end{Bmatrix} \begin{Bmatrix} A \\ B \\ C \end{Bmatrix} = \begin{pmatrix} \Delta h_1 & \Delta h_2 & \cdots & \Delta h_N \\ S_0 & S_1 & \cdots & S_{N-1} \\ 1 & 1 & \cdots & 1 \end{pmatrix} \begin{Bmatrix} \delta S_1 \\ \delta S_2 \\ \vdots \\ \delta S_N \end{Bmatrix} \quad \text{(v)}$$

Here by replacing:

$$D = \begin{Bmatrix} \Delta h_1 & S_0 & 1 \\ \Delta h_2 & S_1 & 1 \\ \vdots & \vdots & \vdots \\ \Delta h_N & S_{N-1} & 1 \end{Bmatrix}$$

then we have:

$$\begin{pmatrix} \Delta h_1 & \Delta h_2 & \cdots & \Delta h_N \\ S_0 & S_1 & \cdots & S_{N-1} \\ 1 & 1 & \cdots & 1 \end{pmatrix} = D^T$$

In addition, replacement as

$$x = \begin{Bmatrix} A \\ B \\ C \end{Bmatrix}, \; y = \begin{Bmatrix} \delta S_1 \\ \delta S_2 \\ \vdots \\ \delta S_N \end{Bmatrix}$$

gives:

$$D^T D x = D^T y \quad \text{(vi)}$$

The parameters of A, B and C are given as the solution of Eq. (vi).